Available at www.sciencedirect.com

Metabolism

www.metabolismjournal.com

Pharmacokinetics and tissue distribution of inositol hexaphosphate in C.B17 SCID mice bearing human breast cancer xenografts

Julie Eiseman[a,b,*], Jing Lan[a,b], Jianxia Guo[a,b], Erin Joseph[a], Ivana Vucenik[c]

[a] Molecular Therapeutics and Drug Discovery Program, University of Pittsburgh Cancer Institute, Pittsburgh, PA 15213, USA
[b] Department of Pharmacology and Chemical Biology, School of Medicine, University of Pittsburgh, Pittsburgh, PA 15213, USA
[c] Department of Medical and Research Technology, University of Maryland School of Medicine, Baltimore, MD 21201, USA

ARTICLE INFO

Article history:
Received 23 December 2010
Accepted 28 February 2011

ABSTRACT

Inositol hexaphosphate (IP_6) is effective in preclinical cancer prevention and chemotherapy. In addition to cancer, IP_6 has many other beneficial effects for human health, such as reduction in risk of developing cardiovascular disease and diabetes and inhibition of kidney stone formation. Studies presented here describe the pharmacokinetics, tissue distribution, and metabolism of IP_6 following intravenous (IV) or per os (PO) administration to mice. SCID mice bearing MDA-MB-231 xenografts were treated with 20 mg/kg IP_6 (3 μCi per mouse [^{14}C]-uniformly ring-labeled IP_6) and euthanized at various times after IP_6 treatment. Plasma and tissues were analyzed for [^{14}C]-IP_6 and metabolites by high-performance liquid chromatography with radioactivity detection. Following IV administration of IP_6, plasma IP_6 concentrations peaked at 5 minutes and were detectable until 45 minutes. Liver IP_6 concentrations were more than 10-fold higher than plasma concentrations, whereas other normal tissue concentrations were similar to plasma. Only inositol was detected in xenografts. After PO administration, IP_6 was detected in liver; but only inositol was detectable in other tissues. After both IV and PO administration, exogenous IP_6 was rapidly dephosphorylated to inositol; however, alterations in endogenous IPs were not examined.

1. Introduction

Inositol hexaphosphate (IP_6, InsP_6, or phytic acid) and inositol, naturally occurring carbohydrates, are widely distributed among plants. Inositol hexaphosphate is found in concentrations from 0.4% to 6.0% in rice, corn, beans, whole-grain cereals, nonrefined cereals derivatives, and all types of nuts [1,2]. It is also present in mammalian cells and tissues at concentrations that range between 0.01 to 1 mmol/L [3-6]. A 6-carbon inositol ring represents the basic carbohydrate moiety in IP_6 and its lower phosphate derivatives ($IP_{1\text{-}5}$). These various inositol phosphates (IPs) are regulated by complex metabolic cycles of phosphorylation and dephosphorylation by IPs kinases and phosphatases. More phosphorylated IPs with 7 (IP_7) and 8 (IP_8) phosphate groups, inositol pyrophosphates, have also been identified [7]. The intracellular higher inositol phosphates (IP_4-IP_6) are synthesized from *myo*-inositol to IP_3 by various kinases. Specific kinases have been identified in mammalian cells that phosphorylate IP_5 at the D2 position on the inositol ring to produce IP_6 [8,9]. Intracellular IP_5 and IP_6 can be further phosphorylated to diphosphorylated PP-IP_4 and

Each author's contribution: Eiseman Julie and Vucenik Ivana: design, implementation, analysis of data, and writing manuscript; Jing Lan: HPLC methods development and analysis; Jiaxia Guo: HPLC analysis, processing of samples, and assisted in data analysis and in writing manuscript; Erin Joseph: dosing and observations on mice, PK sampling, and assistance with manuscript preparation.

* *Corresponding author*. University of Pittsburgh Cancer Institute, Hillman Cancer Center, Research Pavilion, 5117 Centre Ave, Pittsburgh, PA 15213, USA. Tel.: +1 412 623 3239; fax: +1 412 623 1212.
E-mail address: eisemanj@msx.upmc.edu (J. Eiseman).

0026-0495/$ – see front matter © 2011 Elsevier Inc. All rights reserved.
doi:10.1016/j.metabol.2011.02.015

PP-IP_5, respectively. Only the diphosphorylated PP-IP_5 has been characterized, and the diphosphate group is on the 5-carbon of the inositol ring [10,11]. The concentrations of these higher inositol phosphates appear to be tightly controlled through feedback [11]. Although the roles of endogenous IPs have not been completely characterized, IP_5 and IP_6 appear to play a role in numerous cellular processes. For example, IP_6 has been shown to bind to the clathrin assembly proteins and inhibit clathrin cage assembly, to inhibit serine and threonine phosphatases, to alter calcium channel signaling, and to stimulate nonhomogeneous DNA end joining of double-strand breaks by binding to Ku [12,13]. IP_5 and IP_6 also serve as an intracellular reservoir from which the polyphosphorylated inositols are synthesized.

Despite limited information on the functions of IP_6 in animals, numerous studies have demonstrated that IP_6 has chemopreventive as well as therapeutic anticancer activity in a wide variety of tumor types, both in vitro and in vivo [14,15]. In vitro studies have shown that IP_6 inhibits growth and induces differentiation and apoptosis of human breast, colon, prostate, and liver cancer cells. IP_6 reverses the transformed phenotype of HepG2 liver cancer cells [14,15]. The concentrations of IP_6 required to produce anticancer actions in cell culture tend to be in the high micromole per liter or millimole per liter range. For example, in in vitro studies with breast cancer cell lines, 0.5 to 2 mmol/L IP_6 concentrations were required [14,15].

In the first in vivo studies, the effectiveness of IP_6 to prevent cancer was evaluated after administration of IP_6 in the drinking water. The exogenous 1% IP_6 in drinking water 1 week before or 2 weeks after administration of azoxymethane inhibited the development of large intestinal cancer in Fisher 344 rats [16]. In the same model, administration of 2% IP_6 in the drinking water was effective even when the treatment had begun 5 months after carcinogen initiation. Compared with untreated rats, animals on IP_6 had 27% fewer tumors [17]. These findings pointed towards the possible therapeutic use of IP_6. A consistent, reproducible, and significant inhibition of mammary cancer by IP_6 was shown in experimental models chemically induced by either 7,12-dimethylbenz[*a*]anthracene or *N*-methylnitrosourea; the effect was seen on tumor incidence, tumor size, and tumor multiplicity [18]. With regard to the in vivo efficacy of IP_6 against prostate cancer, recent studies demonstrated that continuous administration of 2% IP_6 in the drinking water, beginning 24 hours after subcutaneous implantation of DU-145 prostate cancer cells, resulted in a 66% decrease in tumor burden [19]. In addition, chemopreventive efficacy of IP_6 was observed against prostate tumor growth and progression in TRAMP mice [20]. Furthermore, IP_6 was able to inhibit growth of rhabdomyosarcoma tumor xenografts, regress liver cancer xenografts, inhibit the growth of murine fibrosarcoma, and prevent lung metastases [14,15].

The pharmacokinetics of exogenously administered IP_6 has not been well characterized. When rats were treated with [^{3}H]-*myo*-IP_6 intragastrically, 79% of the radioactivity was absorbed and was widely distributed to tissues; however, most of the radioactivity in plasma and urine was in the form of inositol or inositol monophosphate, suggesting dephosphorylation of IP_6 [21]. In vitro, [^{3}H]-IP_6 was rapidly absorbed and metabolized by murine and human malignant cells [22]. In a clinical trial where subjects were maintained on IP_6-restricted diet for 2 weeks, the ingestion of 1 g Na-phytate resulted in peak IP_6 plasma concentrations at 4 hours that were 3-fold higher than baseline concentrations [3]. Urinary excretion of IP_6 was similar following different preparations of IP_6 [3]. When rats on an IP_6-restricted diet were challenged with IP_6, brain concentrations of IP_6 increased dramatically; but the concentrations of lower inositols were not affected [4]. IP_6 concentrations in the human breast cancer cell line, MDA-MB-231, were not altered following exposure to IP_6 for 1 hour in the medium, but concentrations of lower inositols increased about 2-fold [4,5].

The uptake of extracellular IP_6 is still controversial. Because IP_6 is a highly charged molecule at physiological pH, it does not readily cross cell membranes [23,24]. Using colchicine, an inhibitor of pinocytosis, Ferry et al [25] suggested that in vitro extracellularly applied IP_6 entered HeLa cells pinocytotically and is further dephosphorylated into lower IPs. To understand the mechanism of IP_6 anticancer action, it is important to address the doses used in in vitro and in vivo experiments and to examine the pharmacokinetics of exogenously administered IP_6. The studies presented here describe the plasma pharmacokinetics and tissue distribution of [^{14}C]-uniformly ring-labeled IP_6 following both intravenous (IV) and oral administration to C.B-17 SCID mice bearing MDA-MB-231 breast cancer xenografts. In the studies reported here, the animals were fasted overnight to prevent large amounts of food in their stomachs from interfering with absorption of IP_6. These mice, however, were not placed on a restricted diet, such as AIN-76, with very low concentrations of IP_6. The bioavailability of IP_6 following oral administration was determined in mice receiving a standard diet, and it was assumed that these animals had normal levels of endogenous IP_6 and lower IPs.

2. Materials and methods

2.1. *Chemicals*

Unlabeled phytic acid, K, Mg salt (95% pure) was purchased from Sigma Aldrich (St Louis, MO), whereas uniformly ring-labeled [^{14}C]-phytic acid (IP_6, Mg^{++} K^+ salt, 1 mCi, 2 mCi/mL, specific activity: 250 mCi/mmol, 99% radiochemical purity, 99% chemical purity) was synthesized by American Radiolabeled Chemicals (St Louis, MO). [^{3}H]-labeled lower inositol phosphates and inositol were purchased from NEN, PerkinElmer (Waltham, MA) and used as standards for the radioactive assay.

2.2. *Mice*

C.B-17 SCID female mice (4-6 weeks of age, specific pathogen-free) were purchased from Taconic Farms (Germantown, NY) and allowed to acclimate to the animal facility at the University of Pittsburgh for at least 1 week before initiation of study. Mice were housed in microisolator caging and allowed irradiated food (Prolab ISOPRO 3000; PMI Nutrition International, Brentwood, MO) and autoclaved water ad

libitum except on the evening before dosing, when all food was removed and the animals were fasted overnight. Animal rooms were maintained at 25°C ± 2°C on a 12-hour light/dark cycle and had at least 12 air changes per hour. All animals were handled in accordance with the *Guide to the Care and Use of Laboratory Animals* (National Research Council, 1996) and on a protocol approved by the University of Pittsburgh Animal Care and Use Committee. Sentinel mice (CD1 mice, housed in cages that contained 20% bedding removed from the study mice at cage change) were maintained in the room housing the study mice and were tested for specific pathogens by murine antibody profile testing (Charles River, Boston, MA). Sentinel mice remained free of pathogens throughout the study period, indicating that the study mice were free of specific pathogens as well. MDA-MB-231 human breast cancer cells were obtained from ATCC (Manassas, VA) and cultured in RPMI 1640 medium with 10% heat-inactivated bovine serum and 10 μg/mL gentamicin in 5% CO_2 and 95% humidity. Cells (5×10^6 per mouse) were implanted subcutaneously on the right flank of passage mice. When the tumors in the passage mice reached approximately 500 mm^3 by digital caliper, the tumors were harvested aseptically and cut into approximately 25-mg fragments. The fragments were implanted aseptically on the right flanks of study mice. When the tumors in the study mice reached between 400 and 1500 mm^3, mice were stratified to time point groups. Mice were dosed with 0.01 mL/g body weight of [^{14}C]-IP_6 and unlabeled IP_6 such that each mouse received 20 mg/kg IP_6 and 0.150 mCi/kg in phosphate-buffered saline adjusted to pH 7.2. For the IV study, mice were administered IP_6 by lateral tail vein injection over 60 seconds; and 3 mice per time point were euthanized by CO_2 inhalation at the following time points: 5, 10, 15, 30, 45, 60, 120, 240, 360, 960, and 1380 minutes after IP_6 dosing and 5 minutes after vehicle administration (0.01 mL/g body weight phosphate-buffered saline, pH 7.2). For the per os (PO) study, mice were administered IP_6 using 20-gauge 1-1/2 in gavage needles; and 2 mice per time point were killed at 5, 10, 15, 30, 45, 60, 120, 240, 360, 960, and 1440 minutes after IP_6 and 5 minutes after PO vehicle administration. Blood was collected by cardiac puncture and centrifuged at 13 000*g* for 4 minutes to obtain plasma and packed red blood cells. The following tissues were collected at each time point: liver, kidneys, spleen, heart, lungs, brain, fat, skeletal muscle, and tumor. Tissues were immediately weighed and snap frozen in liquid nitrogen. All samples were stored at –70°C until analysis.

2.3. Sample preparation

Tissues were homogenized in 3 vol of 10 mmol/L $NH_4H_2PO_4$. To 200 μL of the homogenate or plasma, 10 μL of [^{3}H]-IP_4, internal standard (3000 disintegrations per minute [dpms]) and 67 μL of 20% trichloroacetic acid were added to yield a final concentration of 5% trichloroacetic acid. The samples were vortexed for 15 seconds at setting 5 (Vortex Genie; Scientific Industries, Springfield, MA). The samples were then centrifuged at 13 000*g* for 5 minutes, and the supernatants were transferred to glass tubes and dried under a stream of nitrogen gas (Valley Gas, Pittsburgh, PA). After drying, the samples were suspended in 300 μL of mobile phase buffer A (10 mmol/L $NH_4H_2PO_4$, pH 3.5), vortexed for 15 seconds at setting 5, transferred to microcentrifuge tubes, and centrifuged at 13 000*g* for 5 minutes. After centrifugation, the samples were transferred to high-performance liquid chromatography (HPLC) vials; and 100 μL of the sample was injected into the HPLC system.

2.4. HPLC instrument and method

The HPLC system was a Beckman Gold HPLC Programmable Gradient System with IN/US Radioactivity Detection and consisted of a Beckman 508 Autosampler, 128 Gradient Solvent Delivery module, SS420× interface, 32-karat software, radioactive detector β-RAM, model 3 with flow cell (IN/US Systems, Tampa, FL). The column was an anion exchange column SAX (6.2 mm ID × 80 mm) (Agilent Technologies, Palo Alto, CA) with a Reliance cartridge guard column (4.6 mm ID × 12.5 mm, Agilent Technologies). The scintillation fluid used was IN-FLOW Tru-Count Scintillator (IN/US System) and was mixed at a ratio of 1:3 mobile phase to scintillation fluid. Efficiency of detection was 34% for [^{3}H]-and 94% for [^{14}C]. Data analysis was done using Laura Lite 3 Software (Version 3, IN/US Systems, Tampa, FL).

To determine the relative retention time of the various inositol phosphates, standards [^{3}H]-Ins, [^{3}H]-IP_1, [^{3}H]-IP_2, [^{3}H]-IP_3, [^{3}H]-IP_4, [^{3}H]-IP_5, and [^{3}H]-IP_6 (PerkinElmer Life Sciences) were analyzed with each assay. The HPLC method was taken from York et al [26]. The mobile phase was a linear gradient from 100% 10 mmol/L NH_4PO_4 (pH 3.5) to 1 mol/L NH_4PO_4 (pH 3.5) over 18 minutes; 100% 1 mol/L NH_4PO_4 was held for 5 minutes and then decreased to 10 mmol/L NH_4PO_4. The radioactivity detector recorded from 0 to 24 minutes for each run, and the cycle time for the autosampler was 39 minutes for each run to allow return to the initial mobile phase conditions. The retention times of the various inositol phosphate standards were as follows: [^{3}H]-Ins, 2.5 minutes; [^{3}H]-IP_1, 5.5 minutes; [^{3}H]-IP_2, 8.5 minutes; [^{3}H]-IP_3, 11 minutes; [^{3}H]-IP_4, 14 minutes; [^{3}H]-IP_5, 16.5 minutes; and [^{3}H]-IP_6, 20 minutes. The recovery of 3000 dpms [^{14}C]-IP_6 in plasma was 71% through the extraction method, and the recovery of 30 000 dpms [^{16}C]-IP_6 through the extraction method was 84%. The lower limit of quantitation was 300 dpms [^{14}C]-IP_6. The percentages of coefficient of variation for spiked [^{14}C]-IP_6 in plasma at 3000 and 30 000 dpms were less than 15%.

2.5. Noncompartmental pharmacokinetic analysis

IP_6 and inositol exposure (area under the concentration time curves [AUCs]) of plasma and tissues following administration of 20 mg/kg IP_6 (containing 3 μCi per mouse [^{14}C]-uniformly ring-labeled IP_6) to the mice was calculated using the Lagrange function [27] as implemented by the LAGRAN program [28]. The AUCs were also calculated using the trapezoidal method to evaluate agreement between the 2 methods.

3. Results

3.1. Determination of IV maximum tolerated single dose

C.B-17 SCID mice bearing MDA-MB-231 xenografts were administered IV doses of unlabeled IP_6. The mouse given 100 mg/kg IP_6 convulsed and died within 5 minutes of

dosing. Five mice were administered 40 mg/kg. One of these mice convulsed following the administration, whereas the other 4 animals had difficulty walking and were disoriented for at least 30 minutes after dosing. An additional 5 mice were given 25 mg/kg IP_6, and these animals had no untoward effects following administration. Based on these studies, 20 mg/kg IP_6 was chosen for the pharmacokinetic studies of IP_6.

3.2. *IV pharmacokinetic study*

Following IV administration of unlabeled and [^{14}C]-IP_6, peak plasma IP_6 concentrations occurred at 5 minutes, the earliest time point sampled, decreased rapidly, and were not detectable after 45 minutes (Fig. 1A, B; Table 1). Similarly, lower inositol phosphates IP_5, IP_4, and IP_3 were detectable in plasma at 5 minutes, but not detectable beyond 45 minutes after dosing. IP_5 peaked at 5 minutes, whereas IP_4 and IP_3 peaked at 10 minutes after dosing with IP_6. IP_2 and IP_1 were not detectable in plasma until 10 minutes and were less than the detection limit at 60 minutes. In contrast, inositol peak plasma concentrations, 1.37 ± 0.16 μmol/L, were not reached until 360 minutes after administration of IP_6 and

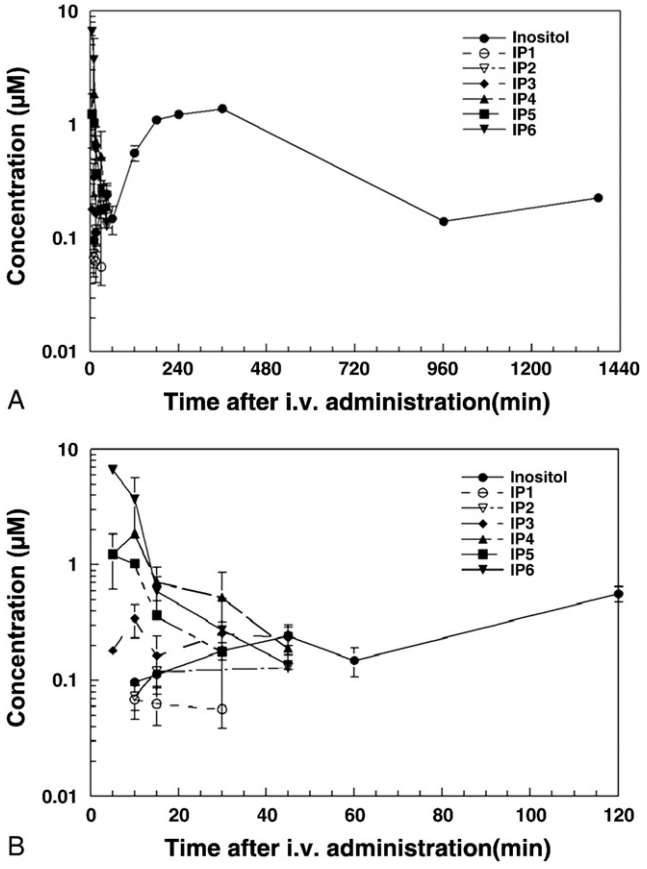

Fig. 1 – Plasma concentration time curve of [^{14}C]-IP_6 and [^{14}C]-metabolites following slow bolus IV injection of mice with 20 mg/kg IP_6 (containing 3 μCi per mouse [^{14}C]-uniformly ring-labeled IP_6). A, Time course for 0 to 1440 minutes after dosing. B, Time scale expanded to show early time points from 0 to 120 minutes.

Table 1 – Concentrations and AUCs of IP_6 in plasma and tissues of C.B-17 SCID mice bearing MDA-MB-231 tumors injected IV With 30.3 μmol/kg IP_6

Time (min)	Plasma (μmol/L)	Liver (μmol/L)	Kidney (μmol/L)	Tumor (μmol/L)	Lung (μmol/L)	Heart (μmol/L)	Spleen (μmol/L)	Fat (μmol/L)	Brain (μmol/L)	GI tract (μmol/L)	Sk muscle (μmol/L)	RBC (μmol/L)
5	6.62 ± 0.38	96.34 ± 11.63	4.90 ± 0.96	ND	3.27 ± 0.04	6.98 ± 2.69	6.45 ± 0.68	1.23 ± 0.30	0.55 ± 0.14	3.76 ± 1.06	1.73 ± 0.25	94.16 ± 57.54
10	3.68 ± 1.98	130.11 ± 2.35	6.51 ± 0.92	ND	22.43 ± 4.79	3.55 ± 0.30	8.80 ± 2.80	1.08 ± 0.35	6.29[a]	6.88 ± 3.10	2.01 ± 0.64	3.21 ± 3.04
15	0.60 ± 0.20	86.21 ± 11.39	0.89 ± 0.44	ND	11.27 ± 3.47	3.10 ± 1.74	6.67 ± 0.74	3.39 ± 0.37	ND	3.67 ± 0.78	1.76 ± 0.71	0.13[a]
30	0.27 ± 0.24	71.68 ± 19.72	1.39 ± 1.39	ND	10.94 ± 3.95	1.42 ± 0.70	3.31 ± 1.73	0.99 ± 1.12	ND	3.39 ± 0.72	1.33 ± 0.49	ND
45	0.14 ± 0.24	92.06 ± 17.11	2.0 ± 1.13	ND	7.90 ± 2.57	2.81 ± 2.16	3.34 ± 0.45	0.77 ± 0.90	ND	3.83 ± 0.80	1.85 ± 1.06	ND
60	ND	114.45 ± 1.61	3.18 ± 1.61	ND	12.02 ± 2.57	2.77 ± 1.10	3.49 ± 0.71	0.77 ± 0.09	ND	4.39 ± 0.80	1.75 ± 0.34	ND
120	ND	32.82 ± 9.97	1.87 ± 0.68	ND	4.03 ± 1.67	0.60 ± 0.36	2.73 ± 0.89	1.82[a]	ND	2.98 ± 0.19	1.82[a]	ND
180	ND	7.84 ± 2.33	1.16 ± 0.31	ND	3.02 ± 1.75	1.55 ± 0.94	1.74 ± 0.68	0.48[a]	ND	2.70 ± 0.19	1.44[a]	ND
240	ND	6.35 ± 0.83	0.76 ± 0.37	ND	ND	0.65 ± 0.21	2.54 ± 0.34	ND	ND	2.68 ± 0.19	2.02 ± 1.08	ND
360	ND	2.61 ± 1.65	ND	ND	ND	ND	2.53 ± 0.80	ND	ND	ND	ND	ND
960	ND	ND	ND	ND	ND	ND	1.31 ± 1.10	ND	ND	ND	ND	ND
1380	ND	0.12 ± 0.05	ND	ND	ND	ND	1.64 ± 1.03	ND	ND	ND	ND	ND
AUC_p	56.8	9321.5	453.5	ND	126.2	415.8	2802.3	210.9	14.1	796.1	397.9	548.0

Each value is the mean ± the standard deviation of 3 samples. AUC_p is the partial area under the concentration time curve, expressed as micromoles per liter·minute. GI indicates gastrointestinal; ND, not detected.

[a] Value is from one mouse.

were still greater than 0.1 μmol/L at the last time point sampled, 1380 minutes.

Red blood cell (RBC) concentrations of IP_6 at 5 minutes were 14-fold higher than concomitant plasma concentrations at 5 minutes (94.16 ± 57.54 μmol/L), were equivalent to plasma concentrations of IP_6 at 10 minutes, and were less than the detection limit of the assay at 15 minutes after dosing and at later time points (Table 1).

Following IV administration of IP_6, only IP_6 and inositol were detected in liver (Fig. 2, Tables 1 and 2). Liver concentrations of IP_6 were 10- to 20-fold higher than those in plasma at the corresponding times (Table 1). The peak IP_6 concentration in liver, 130.11 ± 2.35 μmol/L, occurred at 10 minutes after administration of IP_6; and concentrations remained constant for the first 60 minutes. The concentration of IP_6 then declined; and at 1380 minutes after dosing, the concentration of IP_6 was 0.12 ± 0.05 μmol/L. In liver, inositol concentrations were detected at 15 minutes after IP_6 administration and peaked at 240 minutes. Inositol concentrations were still detectable at 1380 minutes after IP_6 administration and were at least 10-fold higher than IP_6 concentrations in liver.

In the tumor xenografts, no radioactive IPs were detected until 120 minutes, when inositol was detected (Fig. 3). Inositol concentrations then rose to a peak concentration at 360 minutes, the same time as the maximum inositol in plasma.

Spleen contained detectable concentrations of IP_6 throughout the study (Table 1). Peak IP_6 concentrations occurred at 10 minutes and remained detectable until 1380 minutes. Similarly, inositol concentrations were detectable in spleen beginning at 10 minutes after dosing with IP_6 and remained detectable throughout the study (Table 2). None of the lower inositol phosphates were detectable in the spleen.

Concentrations of IP_6 in kidney and lung were higher than plasma concentrations for the early time points except 5 minutes; and peak IP_6 concentrations were achieved at 10 minutes, 6.51 ± 0.92 and 22.43 ± 4.79 μmol/L, respectively (Table 1). IP_6 was detected out to 240 minutes in the kidneys and to 180 minutes in the lungs. In the lungs, IP_5 was also detectable between 60 and 180 minutes, although the concentrations were lower than the concentrations of IP_6 at these

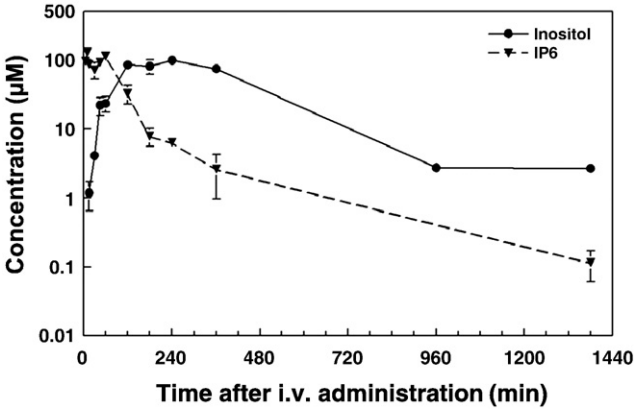

Fig. 2 – Concentration time curve of [^{14}C]-IP_6 and [^{14}C]-inositol in liver following slow bolus IV injection of mice with 20 mg/kg IP_6 (containing 3 μCi per mouse [^{14}C]-uniformly ring-labeled IP_6).

Table 2 – Concentrations and AUCs of inositol in plasma and tissues of C.B-17 SCID mice bearing MDA-MB-231 tumors injected IV With 30.3 μmol/kg (20 mg/kg) IP_6

Time (min)	Plasma (μmol/L)	Liver (μmol/L)	Kidney (μmol/L)	Tumor (μmol/L)	Lung (μmol/L)	Heart (μmol/L)	Spleen (μmol/L)	Fat (μmol/L)	Brain (μmol/L)	GI tract (μmol/L)	Sk muscle (μmol/L)	RBC (μmol/L)
5	ND	ND	0.47 ± 0.24	ND	1.73 ± 0.19	ND	ND	ND	ND	2.33[a]	ND	ND
10	0.01 ± 0.006	ND	0.48 ± 0.09	ND	2.69 ± 0.99	ND	0.859 ± 0.339	ND	ND	1.71 ± 1.49	ND	ND
15	0.111 ± 0.01	1.17 ± 0.53	0.50 ± 0.09	ND	1.51 ± 0.25	ND	2.25 ± 0.563	ND	ND	2.94[a]	ND	ND
30	0.18 ± 0.03	4.08 ± 0.75	0.61 ± 0.16	ND	2.08 ± 1.32	ND	6.15 ± 2.903	ND	ND	2.41 ± 0.17	ND	ND
45	0.25 ± 0.04	22.01 ± 6.55	1.38 ± 0.31	ND	4.28 ± 0.55	0.36 ± 0.06	9.86 ± 1.572	0.60[a]	ND	2.99 ± 0.11	ND	ND
60	0.15 ± 0.04	23.42 ± 6.12	0.98 ± 0.29	ND	4.72 ± 1.28	0.29 ± 0.14	10.10 ± 1.045	1.00 ± 0.06	ND	3.48 ± 0.29	ND	ND
120	0.56 ± 0.09	84.8 ± 14.31	7.62 ± 1.88	0.07 ± 0.039	10.83 ± 0.24	2.32 ± 0.24	7.20 ± 1.264	1.17 ± 0.02	0.59 ± 0.01	4.16 ± 0.27	1.44[a]	ND
180	1.10 ± 0.04	81.10 ± 19.13	15.14 ± 0.76	0.80 ± 0.08	19.20 ± 1.07	1.11 ± 0.12	5.68 ± 1.137	2.06 ± 0.42	0.95 ± 0.15	5.14 ± 0.88	1.54 ± 0.13	2.45 ± 0.56
240	1.22 ± 0.04	99.00 ± 1.18	19.39 ± 1.86	0.93 ± 0.38	23.01 ± 7.29	1.78 ± 0.63	7.10 ± 0.614	3.19 ± 0.88	1.23 ± 0.12	5.58 ± 0.22	1.55 ± 0.13	3.11 ± 2.45
360	1.37 ± 0.16	74.50 ± 12.10	36.70 ± 7.89	2.39 ± 0.40	27.43 ± 2.50	1.55 ± 0.15	7.00 ± 1.135	4.95 ± 4.29	2.20 ± 0.22	6.83 ± 1.78	2.40 ± 0.49	6.62 ± 5.88
960	0.14 ± 0.01	2.73 ± 0.09	22.12 ± 0.94	1.58 ± 0.80	26.94 ± 1.04	1.81 ± 0.63	2.70 ± 2.894	3.88 ± 3.16	1.03 ± 0.89	4.45 ± 0.59	2.00 ± 0.25	0.017[a]
1380	0.0.23 ± 0.01	2.67 ± 0.45	38.17 ± 4.93	1.79 ± 0.84	29.60 ± 5.38	1.71 ± 0.79	4.97 ± 1.886	4.38 ± 2.18	1.15 ± 0.62	5.15 ± 0.90	2.33 ± 0.28	0.70[a]
AUC_p	886	4380	39324	2580	34965	2177	6921	7197	2497	7084	3024	4539

Each value is the mean ± the standard deviation of 3 samples. AUC_p is the partial area under the concentration curve, expressed as micromoles per liter·minute.
[a] Value is from one mouse.

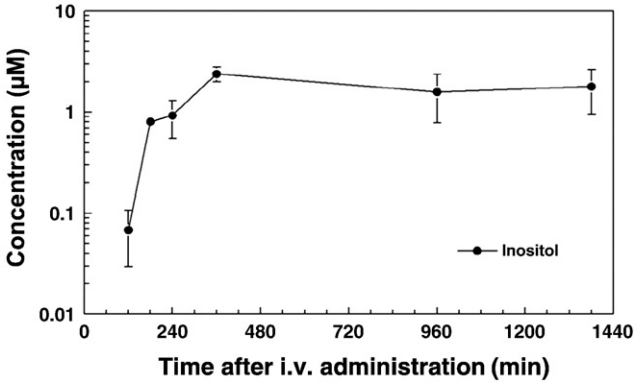

Fig. 3 – Concentration time curve of [^{14}C]-inositol in MDA-MB-231 xenografts following slow bolus IV injection of mice with 20 mg/kg IP_6 (containing 3 μCi per mouse [^{14}C]-uniformly ring-labeled IP_6).

time points (data not shown). In the heart, peak concentrations of IP_6 occurred at 5 minutes after dosing, 6.98 ± 2.69 μmol/L, and were detectable to 240 minutes after dosing. Inositol concentrations in kidney, heart, and lung were higher than the concentrations of IP_6 at all time points beyond 120 minutes (Tables 1 and 2). The exposure of these tissues to inositol, AUC_p, was much greater than the exposure to IP_6.

In brain, IP_6 was only detectable at 5 minutes after dosing; and the concentration of IP_6 was very low compared with plasma or other tissues, 0.55 ± 0.14 μmol/L. Inositol was detectable in brain beyond 120 minutes and remained relatively constant (Tables 1 and 2).

Fat, gastrointestinal tract, and skeletal muscle contained lower concentrations of IP_6 than did plasma at 5 minutes; however, concentrations of IP_6 were detectable for much longer periods of time. Inositol was detected in these tissues at later time points at higher concentrations than IP_6 (Tables 1 and 2).

In contrast to the normal tissues, MDA-MB-231 xenografts did not have detectable concentrations of IP_6; and inositol concentrations slowly increased until a peak concentration of 2.39 ± 0.40 μmol/L was achieved at 360 minutes after dosing (Fig. 3, Tables 1 and 2).

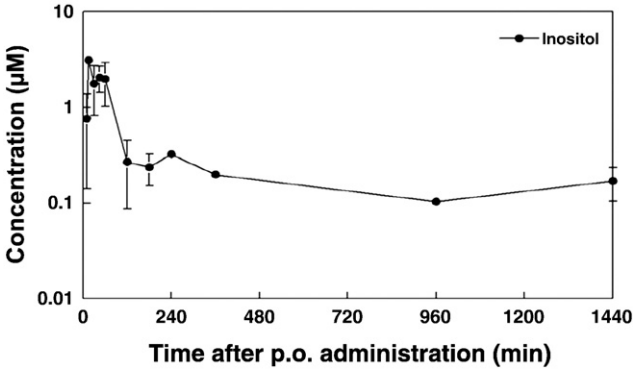

Fig. 4 – Plasma concentration time curve of [^{14}C]-inositol following oral gavage of 20 mg/kg IP_6 (containing 3 μCi per mouse [^{14}C]-uniformly ring-labeled IP_6) to mice.

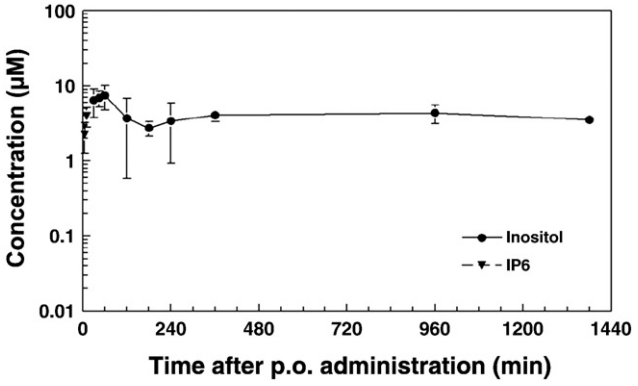

Fig. 5 – Concentration time curve of [^{14}C]-IP_6 and [^{14}C]-inositol in liver following oral gavage of mice with 20 mg/kg IP_6 (containing 3 μCi per mouse [^{14}C]-uniformly ring-labeled IP_6).

Following oral administration of 20 mg/kg IP_6, 2 mice were euthanized at each time point after dosing. No IP_6 was detectable in the plasma of these mice at any of the times after dosing. Only inositol was detected in plasma beginning at 10 minutes after oral administration of IP_6 (Fig. 4). Furthermore, the concentrations of inositol detected in plasma after oral administration were much lower than the concentrations obtained at the same time points after IV administration.

Liver concentrations of IP_6 were detectable after oral administration, but for only the first 15 minutes; and the concentrations of IP_6 were 10-fold lower than those observed after IV administration of IP_6 (Fig. 2 and Table 1 compared with Fig. 5). Inositol was also detected in the liver of mice after oral administration of IP_6; however, the concentrations of inositol after oral administration were approximately 10-fold lower than concentrations observed in liver after IV administration (Figs. 2 and 5). The peak concentration of inositol in MDA-MB-231 xenografts of mice administered PO IP_6 was about 3-fold lower than the peak concentration of inositol in MDA-MB-231 xenografts of mice administered IV IP_6 (Figs. 3 and 6).

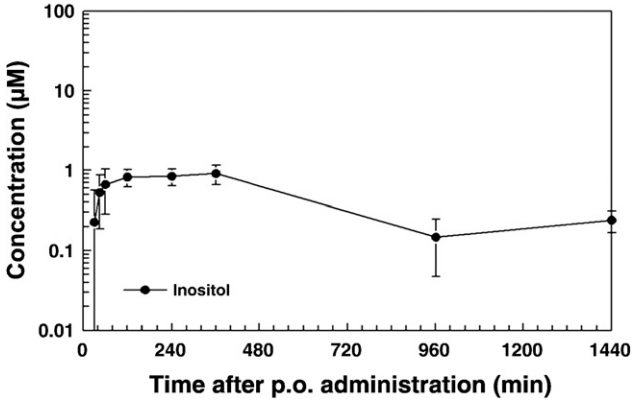

Fig. 6 – Concentration time curve of [^{14}C]-inositol in MDA-MB-231 xenografts following oral gavage of mice with 20 mg/kg IP_6 (containing 3 μCi per mouse [^{14}C]-uniformly ring-labeled IP_6).

Table 3 – Noncompartmental pharmacokinetic analyses of plasma concentration vs time data after administration of IP_6 (30.3 μmol/kg, IV or PO) to C.B-17 SCID mice bearing MDA-MB-231 Xenografts

	$AUC_{0\rightarrow\infty}$ (μmol/(L min)	$t_{1/2}$ (min)	V_{dss}, (mL/kg)	Cl_{tb} (mL/min/kg)
IP_6 IV	57.2	8.1	5056.3	529.1
Inositol IV	3685	365	18896.5	30.1
IP_6 PO	ND	ND	ND	ND
Inositol (PO)	714	1312	51 603	29.1

The plasma IP_6 and inositol concentrations after IV and oral administration were modeled using the Lagrange function, and the data are presented in Table 3. IP_6 was not bioavailable after oral administration to mice. The bioavailability of inositol after oral administration of IP_6 was about 20% of that detected in plasma after IV administration.

Clearance of IP_6 was extremely rapid, 529.1 mL/min/kg, whereas the clearance of inositol was much slower, approximately 30 mL/min/kg, after both IV and oral IP_6 administration.

Urinary excretion of radiolabeled compound accounted for only 2.5% of the intravenously administered dose of IP_6, and 90% of that was in the form of inositol. After oral administration, only inositol was detected in the urine; and it represented only 0.3% of the dose administered to the mice (data not shown).

4. Discussion

The anticancer effects of IP_6 have been reviewed recently by both Vucenik and Shamsuddin [14,15] and Fox and Eberl [29]. From these reviews, it is apparent that the administration of exogenous IP_6 to animals, primarily by oral administration, results in decreased tumor burden or decreased multiplicity of tumors. A number of studies have suggested that the chelating ability of phytic acid may inhibit colon cancer by depriving the cells of needed minerals, including calcium, zinc, iron, and magnesium. Alternatively, the activity of IP_6 most likely is due to its conversion to lower inositols. Of the studies sited, only one by Vucenik et al [30] examined a parenteral route of administration of IP_6, intraperitoneal; and this study demonstrated a reduction in a fibrosarcoma implanted in mice and a decreased number of pulmonary metastases. The IP_6 doses used in vitro in most reports investigating its anticancer action are between 0.1 and 5 mmol/L, with biological effects seen in cell culture mostly at concentrations of 2 to 5 mmol/L [14,15]. In studies in which animals are treated with IP_6, the concentrations formulated in the diet or added to drinking water were up to 15 mmol/L [14-20]. These concentrations are much higher than the concentrations reported in normal rat tissues, which ranged between 10 and 34 μmol/L [5,6]. Very few studies have examined the absorption of IP_6 after oral administration, and we are not aware of any studies that have examined the concentrations of IP_6 after IV administration.

In the current study, mice were acclimated to the standard diet used for immunodeficient mice at the University of Pittsburgh, a diet that is high in grains, with the first 4 ingredients being ground wheat, dehulled soybean meal, wheat middlings, and ground corn (data sheet, www.labdiet.com). Mice were fasted overnight to prevent stomach contents from interfering with the absorption of IP_6; and IP_6 was administered exogenously, each mouse receiving approximately 0.606 μmol of IP_6 by either IV tail vein injection or oral gavage. The oral bioavailability of IP_6 in mice was determined in animals that were fed a standard rodent diet. The resulting tissue concentrations of labeled IP_6 at early time points after IV administration are higher than the endogenous concentrations found in rat tissues except for brain that was reported to contain 32.3 μg/g (48.9 μmol/L) [31]. The liver appeared to accumulate IP_6 and rapidly dephosphorylate it. Peak liver concentrations were approximately 130 μmol/L at 10 minutes but were approximately 0.1 μmol/L at 1380 minutes after administration. In rats, endogenous liver phytic acid concentrations were reported to be between 3.2 and 4.1 μg/g (4.8 and 6.2 μmol/L) [31]. In our study, IP_6 concentrations in most other tissues were less than 10 μmol/L and decreased with time as the concentrations of inositol increased. The concentrations of inositol in tissues in this study are well less than the concentrations reported for endogenous inositol in rats, where brain, liver, and kidney inositol concentrations were reported to be 6.62, 0.57, and 4.51 μmol/g, respectively, much higher than even our peak liver concentrations of 99 μmol/L (99 nmol/g) [32]. It must be noted that the use of a radiolabeled compound mixed with unlabeled compound cannot provide any information about the endogenous intracellular concentrations of IP_6, other inositol phosphates, and inositol. However, to understand what happens to exogenously administered IP_6, the label provided an ideal way to monitor the parent compound and its dephosphorylated forms. It allowed the tracking of the degradation of IP_6 in plasma, which appeared to occur rapidly. Previous studies were performed using [^{3}H]-IP_6. In this study, custom-labeled [^{14}C]-IP_6 was used to avoid concerns of hydrogen exchange. The intermediate inositol phosphates appeared in plasma in the order of the number of phosphates on the sugar, but disappeared rapidly such that only inositol was present 1 hour following IP_6 administration.

The data presented in this study are the first to systematically examine the metabolism of exogenously administered IP_6 in both plasma and tissues of mice bearing tumors. IP_6 was not detected in the tumors at any time after IV administration of IP_6. Inositol was detected in the tumor beginning at 2 hours after IV administration of IP_6 and peaked at 6 hours after administration. At 6 hours, the concentration of inositol in the tumors was about 2-fold higher than that in plasma, but much lower than that observed in most normal tissues.

It appears that IP_6 is dephosphorylated quite rapidly in plasma and also transported to the liver where numerous phosphatases are localized. Because the concentrations of inositol in the liver are higher than those of IP_6 at 2 hours and later time points, the liver may be a major site for the dephosphorylation of intravenously administered IP_6. This dephosphorylation process appears to completely remove the phosphate groups from the sugar because none of the lower inositol phosphates were detected in the liver, whereas the inositol increased as the IP_6 decreased. Similarly, no lower

inositol phosphates were detected in other normal tissues except in the lung. In lung, IP_5 was detected during the first 15 minutes after IV IP_6 administration; however, after 3 hours, only inositol was present as a labeled compound. Thus, it appears that the dephosphorylation of IP_6 occurs rapidly, whereas synthesis of new phosphorylated forms is very slow. After oral administration, only inositol was detected in tissues other than liver. In the liver, IP_6 was detected at concentrations less than 10 μmol/L only at the earliest time points, suggesting that dephosphorylation of orally administered IP_6 occurs rapidly by phytases present in gut bacteria, intestinal mucosa, or the liver.

In rats, radioactivity from [^{3}H]-IP_6 was absorbed from the stomach and distributed through the body [21]. Similarly, radioactivity from [^{3}H]-IP_6 was taken up by cancer cells; and IP_6 was dephosphorylated into inositol phosphates with fewer phosphate groups ($IP_{1\text{-}5}$) [22]. Radioactivity from orally administered IP_6 was detected in tumor tissue distant from the gastrointestinal tract. When radiolabeled IP_6 was given to animals bearing mammary tumors, a substantial amount of IP_6-associated radioactivity (19.7% of all radioactivity recovered in collected tissues) was found in tumor tissue as early as 1 hour after administration, providing at least in part an explanation for the antineoplastic activity of IP_6 at sites distant from the gastrointestinal tract [15]. It was shown that 50% of the radioactivity was excreted in urine within 72 hours; feces accounted for another 10% of radioactivity, suggesting that at least 40% of the IP_6-associated activity was distributed within the animal tissues [21]. When analyzed by ion-exchange chromatography, the radioactivity in the plasma, urine, and tumors was associated with inositol and IP_1 [15]. Similarly, in the present study, after IV administration, only inositol was detected in the tumor xenografts; and the concentrations of radiolabeled inositol increased slowly over the 24 hours and were maintained at approximately 2 μmol/L, much lower that those observed by Grases et al [4]. In the current studies, only about 3% of the intravenously administered dose was excreted in the urine, primarily as inositol, with $IP_{1\text{-}4}$ present in much lower quantities; and less than 0.1% was excreted in the feces. After oral administration, less was excreted in the urine as inositol; and about 10% of the dose was present in the feces, primarily as inositol. These results are similar to those reported by Letcher et al [6], where no IP_6 was detectable in urine of rats.

Using sensitive methods for determination of nonradiolabeled IP_6 in biological fluids, Grases et al [3] studied the pharmacokinetic profile of IP_6 in rats and for the first time in humans. Orally administered IP_6 was excreted in urine; the urinary levels declined when IP_6 was withheld and increased with increasing amounts of ingested IP_6, reaching a peak excretion level that was not further increased by ingestion of additional quantities of IP_6. After 2 weeks of consuming a diet totally deprived of IP_6 (cereal derivatives and other vegetable seeds, legumes, and nuts), the plasma and urinary levels of IP_6 decreased to 75% to 80% of the normal values found in humans [3]. Similar data were observed in rats [5]. After 2 weeks of IP_6-restricted diet, a challenge dose of IP_6 was quickly absorbed, reaching the maximum plasma concentrations 4 hours after ingestion of pure IP_6 as supplement [3]. No urinary excretion of IP_6 was observed until 10 days after returning to normal IP_6-containing diets [3]. A similar relationship between the dietary ingestion of IP_6 and its levels in the biological fluids and tissues was observed in rats [5]. In an additional study, Grases et al [5] demonstrated that when rats were fed an IP_6-deficient diet, plasma IP_6 concentrations fell to 0.026 μmol/L, whereas rats fed diets containing 1% IP_6 maintained plasma concentrations of IP_6 of 0.393 μmol/L, similar to the concentrations found in rats that consumed a diet containing carob germ, a good plant source of IP_6. These concentrations of IP_6 were within the reference range [5]. It may be that IP_6 and lower IPs are absorbed more efficiently when the animals are made deficient by dietary restriction for at least 2 weeks.

Although there are still uncertainties about IP_6 synthesis in vivo in mammalian cells and its uptake, it is clear that IP_6 is a molecule that can be rapidly dephosphorylated to lower IPs. Various lower IPs were found in vitro after extracellular, exogenous application of IP_6 [15,22,25]; and mostly inositol and IP_1 were found after in vivo administration [15,21]. Similarly, the pharmacokinetic study presented here suggests that IP_6 may be a prodrug for inositol, which is not charged and can cross cellular membranes. Inositol may be responsible for the antitumor actions observed in both chemopreventive and efficacy studies of IP_6.

myo-Inositol itself has also been shown to have anticancer activity, although modest. It inhibited colon, mammary, soft tissue, and lung tumor formation [14,15,30,33,34]. The anticancer action of inositol could very well be via phosphorylation to $IP_{1\text{-}6}$ and higher IPs. A recent phase I study of inositol for lung cancer chemoprevention showed that inositol was safe and well tolerated [35]. Inositol has been shown to potentiate anticancer effects of IP_6 observed in vivo and in vitro [14,15,30,33,34,36]. Inositol and IP_6 in combination as an adjunctive therapy in breast cancer patients receiving chemotherapy ameliorated the adverse effects of chemotherapy and preserved quality of life [37].

Our studies also suggest that when animals have sufficient IP_6 in their diets, additional IP_6 is not required and is rapidly dephosphorylated [5]. It is well known that nonruminant animals have lower levels of enzymes to digest phytate; and therefore, a significant part of dietary IP_6 reaches the large intestinal lumen in humans and rodents. Intrinsic phytase naturally present in cereals can partly hydrolyze IP_6 during the digestive process [38-40]. Because the doses used in this pharmacokinetic study (20 mg/kg) were much lower than the doses of 1% to 2% in the diet (~2000 mg/kg//d), the absorption of IP_6 may be different between these studies. Grases et al [5,41] demonstrated that the maximum absorption for IP_6 in rats after oral administration is 20.0 mg/kg//d and that no further absorption occurs even when higher amounts of IP_6 are administered. Thus, the dose of 20 mg/kg IP_6 administered by oral gavage to mice in the study presented here should have been absorbed without saturation of the absorption processes. Although the absorption of IP_6 is saturated at doses greater than 20 mg/kg//d, it is not known whether the inositol derived from these doses is absorbed or eliminated in the feces. The gastrointestinal tract contains numerous phytases that are capable of stripping IP_6 of its phosphates. Future studies need to be conducted to examine whether the efficacy of IP_6 is observed after administration of doses of this agent lower than the 1% to 2% administered in the drinking water and

whether this agent is effective when administered at lower doses by other routes of administration. A question remains as to whether the activity of IP_6 in animal models can be replicated by administration of inositol alone because only inositol was detected in plasma and tumor after oral gavage.

REFERENCES

[1] Harland BF, Oberleas D. Phytate in foods. World Rev Nutr Diet 1987;52:235-59.
[2] Reddy NR, Sathe SK, Salunke DK. Phytates in legumes and cereals. Adv Food Res 1982;28:1-89.
[3] Grases F, Simonet BM, Vucenik I, Prieto RM, Costa-Bauzá A, March JG, et al. Absorption and excretion of orally administered inositol hexaphosphate (IP_6 or phytate) in humans. Biofactors 2001;15:53-61.
[4] Grases F, Simonet BM, Vucenik I, Perelló J, Prieto RM, Shamsuddin AM. Effects of exogenous inositol hexakisphosphate ($InsP_6$) on the levels of $InsP_6$ and of inositol trisphosphate ($InsP_3$) in malignant cells, tissues and biological fluids. Life Sci 2002;71:1535-46.
[5] Grases F, Costa-Bauzá A, Prieto RM. Intracellular and extracellular *myo*-inositol hexakisphosphates ($InsP_6$), from rats to humans. Anticancer Res 2005;25:2593-8.
[6] Letcher AJ, Schell MJ, Irvine RF. Do mammals make their own inositol hexakisphosphate? Biochem J 2008;416:263-70.
[7] Burton A, Hu X, Saiardi A. Are inositol pyrophosphates signaling molecules? J Cell Physiol 2009;220:8-15.
[8] Verbsky JW, Wilson MP, Kisseleva MV, Majerus PW, Wente SR. The synthesis of inositol hexakisphosphate. Characterization of human 1,3,4,5,6-pentakisphosphate 2-kinase. J Biol Chem 2002;277:31857-62.
[9] Shears SB. How versatile are inositol phosphate kinases? Biochem J 2004;377:265-80.
[10] Saiardi A, Caffrey JJ, Snyder SH, Shears SB. The inositol hexakisphosphate kinase family. Catalytic flexibility, and function in yeast vacuole biogenesis. J Biol Chem 2000;275: 24686-92.
[11] Fujii M, York JD. A role for rat inositol polyphosphate kinases rIPK2 and rIPK1 in inositol pentakisphosphate and inositol hexakisphosphate production in Rat-1 cells. J Biol Chem 2005;280:1156-64.
[12] Ye W, Ali N, Bembenek ME, Shears SB, Lafer EM. Inhibition of clathrin assembly by high affinity binding of specific inositol polyphosphates to the synapse-specific clathrin assembly protein AP-3. J Biol Chem 1995;270:1564-8.
[13] Byrum J, Jordan S, Safrany ST, Rodgers W. Visualization of inositol phosphate-dependent mobility of Ku: depletion of the DNA-PK cofactor $InsP_6$ inhibits Ku mobility. Nucleic Acids Res 2004;32:2776-84.
[14] Vucenik I, Shamsuddin AM. Cancer Inhibition by inositol hexaphosphate (IP_6) and inositol: from laboratory to clinic. J Nutr 2003;133:3778S-84S.
[15] Vucenik I, Shamsuddin AM. Protection against cancer by dietary IP_6 and inositol. Nutr Cancer 2006;55:109-25.
[16] Shamsuddin AM, Elsayed AM, Ulah A. Suppression of large intestinal cancer in F344 rats by inositol hexaphosphate. Carcinogenesis 1988;9:577-80.
[17] Shamsuddin AM, Ulah A. Inositol hexaphosphate inhibits large intestinal cancer in F344 rats 5 months after induction by azoxymethane. Carcinogenesis 1989;10:625-6.
[18] Shamsuddin AM, Vucenik I. Mammary tumor inhibition by IP_6: a review. Anticancer Res 1999;19:3671-4.
[19] Singh RP, Sharma G, Mallikajurna GU, Dhanalakshmi S, Agarwal C, Agarwal R. *In vivo* suppression of hormone-refractory prostate cancer growth by inositol hexaphosphate: induction of insulin-like growth factor binding protein–3 and inhibition of vascular endothelial growth factor. Clin Cancer Res 2004;10:244-50.
[20] Komal R, Rajamanickam S, Singh RP, Agarwal R. Chemopreventive efficacy of inositol hexaphosphate against prostate tumor growth and progression in TRAMP mice. Clin Cancer Res 2008;14:3177-84.
[21] Sakamoto K, Vucenik I, Shamsuddin AM. [^{3}H]-phytic acid (inositol hexaphosphate) is absorbed and distributed to various tissues in rats. J Nutr 1993;123:713-20.
[22] Vucenik I, Shamsuddin AM. [^{3}H]-inositol hexaphosphate (phytic acid) is rapidly absorbed and metabolized by murine and human malignant cells *in vitro*. J Nutr 1994;124: 861-8.
[23] Vincent SP, Lehn JM, Lazarte J, Nicolau C. Transport of the highly charged myo-inositol hexakisphosphate molecule across the red blood cell membrane: a phase transfer and biological study. Bioorg Med Chem 2002;10:2825-34.
[24] Teisseire B, Ropars C, Villeréal MC, Nicolau C. Long-term physiological effects of enhanced O_2 release by inositol hexaphosphate-loaded erythrocytes. Proc Natl Acad Sci U S A 1987;84:6894-8.
[25] Ferry S, Matsuda M, Yoshida H, Hirata M. Inositol hexakisphosphate blocks tumor cell growth by activating apoptotic machinery as well as by inhibiting the Akt/NFκB-mediated cell survival pathway. Carcinogenesis 2002;23: 2031-41.
[26] York JD, Odom AR, Murphy R, Ives EB, Wente SR. A phospholipase C–dependent inositol polyphosphate kinase pathway required for efficient messenger RNA export. Science 1999;285:96-100.
[27] Yeh KC, Kwan KCA. Comparison of numerical integrating algorithms by trapezoidal, Lagrange and spline approximation. J Pharmacokinet Biopharm 1978;6:79-98.
[28] Rocci ML, Jusko W. LAGRAN program for area and moments in pharmaco-kinetic analysis. Comput Programs Biomed 1983;16:203-16.
[29] Fox CH, Eberl M. Phytic acid (IP_6), novel broad spectrum anti-neoplastic agent: a systematic review. Complement Ther Med 2002;10:229-34.
[30] Vucenik I, Tomazic VJ, Fabian D, Shamsuddin AM. Antitumor activity of phytic acid (inositol hexaphosphate) in murine transplanted and metastatic fibrosarcoma, a pilot study. Cancer Lett 1992;65:9-13.
[31] March JG, Simonet BM, Grases F. Determination of phytic acid by gas chromatography–mass spectroscopy: application to biological samples. J Chromatogr B Biomed Sci Appl 2001;757: 247-55.
[32] Palmano KP, Whiting PH, Hawthorne JN. Free and lipid *myo*-inositol in tissues from rats with acute and less severe streptozotocin-induced diabetes. Biochem J 1977;167: 229-35.
[33] Shamsuddin AM, Ullah A, Chakravarthy A. Inositol and inositol hexaphosphate suppress cell proliferation and tumor formation in CD-1 mice. Carcinogenesis 1989;10: 1461-3.
[34] Vucenik I, Yang G, Shamsuddin AM. Inositol hexaphosphate and inositol inhibit DMBA induced rat mammary cancer. Carcinogenesis 1995;16:1055-8.
[35] Lam S, McWilliams A, leRiche J, MacAulay C, Wattenberg L, Szabo E. A phase I study of *myo*-inositol for lung cancer chemoprevention. Cancer Epidemiol Biomarkers Prev 2006;15:1526-31.
[36] Schröterová L, Hasková P, Rudolf E, Cervinka M. Effect of phytic acid and inositol on the proliferation and apoptosis of cells derived from colorectal carcinoma. Oncol Rep 2010;23: 787-93.
[37] Bačić I, Družijanić N, Karlo R, Škifić I, Jagić S. Efficacy of IP_6 + inositol in the treatment of breast cancer

patients receiving chemotherapy: prospective, randomized, pilot clinical study. J Exp Clin Cancer Res 2010;29:12.
[38] Sandberg AS, Andersson H. Effect of dietary phytase on the digestion of phytate in the stomach and small intestine of humans. J Nutr 1988;118:469-73.
[39] Rapp C, Lantzsch HJ, Drochner W. Hydrolysis of phytic acid by intrinsic plant and supplemental microbial phytase (*Aspergillus niger*) in the stomach and small intestine of minipigs fitted with re-entrant cannulas. 3. Hydrolysis of phytic acid (IP_6) and occurrence of hydrolysis products (IP_5, IP_4, IP_3 and IP_2). J Anim Physiol Anim Nutr (Berl) 2001;85:420-30.
[40] Schlemmer U, Frølich W, Prieto RM, Grases F. Phytate in foods and significance for humans: food sources, intake, processing, bioavailability, protective role and analysis. Mol Nutr Food Res 2009;53:S330-75.
[41] Grases F, Simonet BM, March JG, Prieto RM. Inositol hexakisphosphate in urine: the relationship between oral intake and urinary excretion. BJU Int 2000;85:139-42.